Am. Inst. Chem.
Eng. Jour.,
New York, Dec. 1962

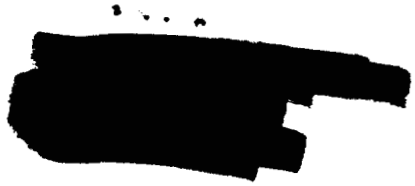

THE GENERATION OF ALKALI-METAL VAPORS IN A 150-KILOWATT FORCED-CIRCULATION FLASH VAPORIZATION FACILITY

By L. R. Nichols, C. H. Winzig, S. M. Nosek, and L. J. Goldman

Lewis Research Center
National Aeronautics and Space Administration
Cleveland, Ohio

INTRODUCTION

During the last few years much interest has been shown in the development of small, lightweight, electrical-power generating systems using nuclear heat as the source of energy. Stationary nuclear-electric powerplants would be used in remote areas and more advanced systems would be used in space flight.

Power levels for space applications range from less than a kilowatt for auxiliary power to the megawatt level for propulsion of manned space vehicles. The nature of these applications demands reliable, unattended operation for as long as a few years.

The conversion of nuclear energy to electrical power can be attained indirectly by turbine-generator units, operating in a closed thermodynamic gas or vapor cycle. Heat is added to the working substance from the energy source and waste heat is rejected from the working fluid by radiation to the space environment. The Rankine vapor cycle using an alkali metal as the working fluid is promising for use in a manned space power system.

Current engineering knowledge and practice and forseeable advances in basic and applied engineering indicate that alkali-metal systems exhibiting long-term reliability at temperatures as high as 2200° F will be among the first generation of manned space power systems. A great effort is now underway to rapidly advance the technology of liquid metals for use at these higher temperatures. Experimental work is proceeding to (1) develop new materials of construction and fabrication techniques compatible with the alkali metals; (2) investigate the phenomena associated with heat transfer to the alkali metals during vaporization and condensation; (3) develop durable and efficient rotating components; and (4) investigate system control and general operational problems by the operation of pilot facilities.

This paper is a summary of the design and initial operational performance of a pilot facility using sodium as the working substance. The forced circulation, liquid-vapor, alkali-metal system consists of two main interconnected processes. The primary system is used to investigate the feasibility of generating saturated metallic vapor by the flash vaporization of compressed liquid sodium and subsequent separation of the saturated phases. Particular interest is directed to possible process instabilities introduced by the large variation of vapor pressure with temperature of the alkali metals. The secondary system is used to study the expansion and flow characteristics of saturated sodium vapor. The vapor is passed through a nozzle to obtain critical weight-flow information and to study the expansion process of metallic vapors. Such information is of both theoretical and practical interest in the

design and operation of vapor turbines. The facility provides a dynamic system for the evaluation of instrumentation components. From such an operation, component and general process reliability and durability data are also obtained.

DESCRIPTION OF SYSTEM

Thermodynamic Cycle and Criteria of Design

The thermodynamic cycle of the sodium flash-vaporization process is shown on the enthalpy-entropy diagram in figure 1. Figure 2 is a schematic drawing of the system that indicates the major components and peak design parameters. Thermodynamic processes are bounded by the noted state points.

The process is designed to circulate up to 50 gallons per minute (19,000 lb/hr) of molten sodium in the primary system. Saturated liquid from a liquid-vapor separator at temperatures up to 1620° F (15 psia) is compressed and passed through the main heater where a maximum of 150 kilowatts of power is added to the sodium by electrical resistance heating, which simulates thermal energy from a nuclear source. Eighty-five percent of the heat is generated directly in the liquid by impressing up to 18 volts and 10,000 amperes single-phase alternating current to the main heater pipe. Maximum sodium temperature at peak design is 1700° F, state 1. A concentric orifice located at the outlet of the heater allows compression of the liquid sodium to suppress boiling within the heater. Decompression of the liquid, due to flow through the orifice, allows fractional flash vaporization, and the two-phase mixture, state 2, flows to the separator. Up to 300 pounds per hour of saturated vapor

from the separator, state 3, is expanded through a convergent nozzle (which simulates a turbine and limits the sodium-vapor mass-flow rate) to state 4. In the vapor chamber the velocity head is converted to enthalpy and superheated vapor results, state 5. Desuperheating and condensing in the air-cooled condenser provides saturated liquid, state 6. Heat losses from the accumulator results in slightly subcooled condensate, state 6'. The condensate is compressed by the secondary pump to state 7 and mixed with the saturated liquid from the separator, state 3', which results in a slightly subcooled liquid, state 8. Compressed liquid from the primary pump at state 9 is heated prior to flashing from state 1 to complete the cycle. During operation the system contains 200 pounds of sodium.

Mechanical

The two-phase sodium facility is composed of three process subsystems: (1) primary system, (2) secondary system, and (3) oxide control and indicating system as shown schematically in figure 2. An isometric drawing is shown in figure 3. All piping is AISI type 316, seamless, stainless steel, schedule 40, with butt-welded joints. The vessels are fabricated from pipe sections with ASME butt-welded closures. Packless, bellows sealed valves are used in the system. All welds are made by the tungsten inert arc process and are dye penetrant and radiographically inspected. The entire facility is helium-mass spectrometer leak-checked to ensure leak tightness.

All vessels and the tee connecting the primary and secondary systems are anchored to the supporting framework. Steel cables support the piping, and adjustable spring-loaded cables support the pumps and valve

actuators. All process piping and vessels are covered with 5 inches of thermal insulation.

The separator is 14 inches in diameter by 48 inches long. An inventory of 1 cubic foot of liquid is maintained in the hot well of the vessel to provide suction head for the primary pump. The liquid effluent from the separator passes through $2\frac{1}{2}$-inch pipe and is combined with condensate from the secondary system. The rate of flow is measured by the primary magnetic flowmeter. The flow is compressed by a two-stage electromagnetic conduction pump and is passed through $2\frac{1}{2}$-inch pipe to the main heater. The heater is a 40-foot length of $1\frac{1}{2}$-inch pipe coiled as shown in figure 3. The electrical taps located at the center of the heater serve as a common junction for the top and bottom halves of the heater, which are connected as a parallel electrical circuit. From the heater the sodium flows through an orifice into a 10-foot length of 4-inch pipe where flashing occurs; from there the mixture passes to the separator.

The vapor outlet from the separator is a short length of 4 inch pipe filled with wire mesh, which serves as a demister. From the demister vapor flows through 3-inch pipe to a convergent nozzle with a 0.775-inch-diameter throat. The nozzle effluent flows directly into the vapor chamber, which is 12 inches in diameter and 18 inches long. This vessel is provided for mounting erosion specimens or research vehicles to be tested in a vapor environment. Three-inch pipe passes the vapors to the air-cooled condenser, which consists of eight U-shaped loops of 1-inch finned tubing that connect the horizontal 3-inch headers.

One-half inch pipe drains the saturated condensate from the condenser to the accumulator, which is 12 inches in diameter by 30 inches long. Liquid from the accumulator is compressed by an electromagnetic pump and measured by the secondary magnetic flowmeter. The secondary flow is joined with the separator liquid effluent in a $2\frac{1}{2}$-inch tee.

The oxide control and indicating system is designed to remove sodium oxide from the system by both a "hot trap" and a "cold trap" and to measure the concentration of the oxide by a plugging valve. The corrosion of containment materials by liquid metals is dependent to a great degree on the metal oxide concentration of the liquid. It is desirable that the sodium be completely free of sodium oxide, however; a practical operating limit is to maintain an oxide level below 50 parts per million. Cold trapping of sodium oxide in sodium is based on the solubility-temperature relation. The forced-circulation cold trap used in this system consists of diverting about 2 gallons per minute from the discharge of the primary pump through an economizer and hence to a cooler. The temperature of the cooler effluent is gradually decreased and passed into the cold trap (a 30 in.-length of 8 in.-pipe packed with stainless steel wire mesh) where the excess oxides are precipitated and retained. The sodium is passed through the economizer and returned to the inlet of the pump. The discharge from the cooler can be diverted to the plugging indicator (a packless bellows sealed valve with a serrated plug). When the solubility limit of the oxide is reached, the precipitate plugs the serrations in the valve which, is indicated by a sharp decrease in flow. The temperature of the stream when plugging

occurs is taken to be the oxide saturation temperature. Reference 1 and 2 contain further discussion of cold trapping methods and contain sodium oxide solubility curves. A continuous drag stream of sodium is passed through a 14-inch length of 3-inch pipe filled with titanium crystals. At temperatures above 1200° F the sodium oxide is chemically reduced as it flows through the hot trap.

Electrical

The power system to the main heater consists of (1) an oil immersed contactor, (2) a saturable core reactor and magnetic amplifier, (3) a 240 kilovolt-ampere, 2400/24 volt transformer, and (4) copper buses that interconnect the transformer to the stainless steel buses welded to the main heater.

The auxiliary power system consists of (1) a single-phase, two-pole, 2400 volt load interrupter, (2) a 100 kilovolt-ampere, 2400/480/240 volt transformer, and (3) a power distribution center. The power center provides 480 volts of power for the primary electromagnetic pump and 240 volts of power for the secondary pump, blowers, and the system preheaters.

Since sodium has a melting point of 208° F, the entire facility must be preheated prior to the introduction of molten sodium from the sump. A network of sheathed resistance heaters provides 25 kilowatts of power for preheating.

Instrumentation

Power to the main heater and cooling of the condenser are controlled by conventional recorder-controllers operating on instream thermocouples. The primary flow rate is controlled by manually positioning the autotransformer in the pump power supply.

Chromel-Alumel thermocouples are used to measure system temperatures. Surface-mounted thermocouples are used for monitoring the system during preheating; those used for controlling and monitoring the process are located in instream wells.

Process pressures are measured by null balance, bellows-type transmitters. An inferential-type gage is used to measure pressures below 1000 microns of mercury. The liquid levels in the separator and the accumulator are measured by radiation emitted by cesium 137.

Power to the main heater and pumps is monitored by recording and indicating instruments.

The system is equipped with devices that give an alarm or initiate a control action, or both in the event of faulty process conditions, such as high pressure, high temperature, and a failure in the process piping.

OPERATION

Prior to initial charging of sodium, the facility was preheated to 800° F and outgassed for 48 hours by continuous evacuation. Thereafter during shutdown periods the system is pressurized with high purity argon gas.

During a conventional startup the system is preheated to 300° to 600° F during the evacuation of the argon cover gas to 25 to 50 microns pressure. The system is isolated from the sump vessel by closing the equalizing line valve. Argon gas is used to pressurize the sodium in the sump vessel, and 200 pounds of sodium is forced through the sump valve to the process system.

After the desired primary flow rate is established by positioning the autotransformer of the primary pump, the main heater temperature is raised to 800° F. An oxide concentration of less than 50 parts per million is established by cold trapping. The plugging-indicator valve is used periodically to determine the oxide saturation temperature. The heater outlet temperature is increased 2° to 4° F per minute until the desired temperature is established. The flow of vapor from the separator to the condenser heats the process piping above the preheat temperature, at which time the line heaters are deenergized. When a temperature of 1000° F is attained in the condenser, the condenser temperature controller is activated. The secondary pump is used to maintain the desired liquid level in the separator.

Steady-State Data

Typical steady-state data obtained over the full range of operating severities are listed in table I. Data for each run were recorded after 2 to 10 hours of steady operation. Data are shown for heater outlet temperatures to 1700° F, condensation temperatures to 1495° F, and primary liquid flow rates as great as 18,800 pounds per hour. Measured rates of vapor generation are listed as secondary flow rates. The listed heater outlet, separator, and condenser temperatures are averages of dual measurements. Pressure data are not listed because of the unreliability of the transmitters. Electrical power data are presented as measured at the secondary bus of the 240kilovolt-ampere transformer.

Critical Rates of Vapor Flow

Theoretical critical rates of vapor flow through the convergent nozzle were calculated considering two expansion processes through the nozzle: (1) equilibrium expansion, and (2) supersaturated expansion. Thermodynamic data from reference 3 were used. The calculations are for an isentropic process, and the vapor is assumed to behave as an ideal gas.

Equilibrium expansion. - During an equilibrium expansion of a vapor below the saturated state, condensation progresses continuously, and phase equilibrium exists throughout the expansion process. Here it is assumed that chemical equilibrium between the monatomic and diatomic species of vaporous sodium also exists.

The critical weight flow rate per unit area is determined from the continuity equation

$$\frac{w_s}{A_x} = \frac{V_x}{v_x} \tag{1}$$

At any inlet pressure p_3, various pressure ratios p_x/p_3 are assumed and the corresponding values of V_x/v_x calculated. A plot of V_x/v_x against p_x/p_3 determines the maximum (critical)mass flow rate.

The velocity of the expanding vapor, neglecting inlet velocity, is calculated from

$$V_x = \left[2g_c J(h_{g,3} - h_x)\right]^{1/2} \tag{2}$$

where the enthalpy at state x is determined from

$$h_x = y_x h_{g,x} + (1 - y_x)h_{f,x} \tag{3}$$

and the quality y is obtained from

$$s_3 = s_x = y_x s_{g,x} + (1 - y_x)s_{f,x} \tag{4}$$

The specific volume is calculated from

$$v_x = y_x v_{g,x} + (1 - y_x) v_{f,x} \tag{5}$$

The results are presented as pounds per hour per square inch in figure 4, curve 1, as a function of inlet pressure p_3. The data are described by

$$\frac{w_s}{a_c} = 39.0\ p_3 \tag{6}$$

Supersaturation expansion. - Actual condensation during expansion may be delayed and cause the sodium vapor to be in a metastable or supersaturated state. In this state the vapor is more dense than when in equilibrium at the same pressure. Expansion in this state results in a lower velocity; however, the fractional increase in density is greater than the decrease in velocity, and a greater rate of flow results than for an equilibrium expansion. It is assumed that supersaturation continues beyond the throat of the nozzle.

In the supersaturated case, it is further assumed that the expansion proceeds too rapidly to allow any change in the chemical association of the vapor species, and that throughout the expansion process the molecular weight of the vapor is unchanged from the initial state point.

The ideal weight flow for the supersaturation expansion can be shown to be

$$\frac{w_s}{A_x} = \left\{ 288\ \frac{g_c n p_3}{v_3 (n - 1)} \left[\left(\frac{p_x}{p_3} \right)^{\frac{2}{n}} - \left(\frac{p_x}{p_3} \right)^{\frac{n+1}{n}} \right] \right\}^{1/2} \tag{7}$$

where the expansion is assumed to follow

$$pv^n = \text{Constant} \tag{8}$$

Lack of knowledge of the polytropic constant for sodium vapor necessitates treating the expansion as isentropic and assuming ideal gas behavior.

The isentropic constant k is calculated from the specific heat data for monatomic and diatomic vapor from reference 3, by

$$C_{p,m} = (1 - x)C_{p,Na_1} + xC_{p,Na_2} \tag{9}$$

$$C_{v,m} = C_{p,m} - R \tag{10}$$

$$k = \frac{C_{p,m}}{C_{v,m}} \tag{11}$$

The isentropic constant k for the temperature range of interest here (1300° to 1600° F) varies from 1.56 to 1.53. Using a value of 1.55 the critical pressure ratio can be determined by

$$\frac{p_c}{p_3} = \left(\frac{2}{k+1}\right)^{\frac{k}{k-1}} \tag{12}$$

By using the ideal gas law, equation (7) reduces to

$$\frac{w_s}{a_c} = 368\ p_3\left(\frac{M_{m,3}}{T_3}\right)^{1/2} \tag{13}$$

The mean molecular weight varies from 25.9 to 26.9 over the temperature range of interest, and $(M_{m,3}/T_3)^{1/2}$ varies from 0.121 to 0.114. Using a mean value of 0.118 equation (13) reduces to,

$$\frac{w_s}{a_c} = 43.4\ p_3, \qquad \text{lb/(hr/sq in.)} \tag{14}$$

This equation is plotted in figure 4, curve 2.

Experimental critical vapor flow rates. - From the data in table I and enthalpy data, the vapors generated by the flashing process can be calculated by

$$w_s = y_2 w_p = \left(\frac{h_1 - h_{f,3}}{h_{g,3} - h_{f,3}}\right) w_p \qquad (15)$$

The calculated secondary flow rates are listed in table II. Also listed is the nozzle inlet pressure p_3 and the ratio of the condenser (or receiving pressure) and the nozzle inlet pressure p_6/p_3. The following equation from reference 3 was used to calculate the vapor pressures from temperature data from table I:

$$\log_{10} p = 5.53103 - \frac{8718.30}{T - 83.2} \qquad (16)$$

With the exhaust or receiving pressures equal to or less than the pressure needed to establish critical flow, the rate of flow for the fixed area nozzle is determined by the temperature and pressure at the nozzle inlet. The pressure ratios for runs 10, 11, and 15 are substantially greater than the nominal 0.5 assumed to be the upper limit for critical flow. With the exclusion of these three runs, the data are plotted as curve 3 in figure 4.

The data are fitted with the curve

$$\frac{w_s}{a_c} = 51.46 + 43.75\ p_3 \qquad (17)$$

where the lowest nozzle inlet pressure is 2.5 pounds per square inch absolute (1321° F).

The measured flow rates corresponding to the same runs are listed in table II and plotted in figure 4, curve 4.

Accuracy of experimental results. - Vapor flow rates calculated from equation (15) indicate a flow of 51.46 pounds per hour per square inch at zero nozzle inlet pressure. This is attributed to errors in temperature and primary flow measurements. In addition, error is introduced by questionable enthalpy values, particularly for the vapor phase, which depends on the degree of chemical association.

Sodium vapor, as do the vapors of all the alkali metals, polymerizes to form, presumably, the dimer. The heat of reaction for the dimerization of vaporous sodium

$$2Na_{1(v)} \rightleftharpoons Na_{2(v)} \tag{18}$$

is not accurately known. Thomson and Garelis (3) in their extensive thermodynamic analysis of the reaction used a value of $-\Delta H_0^\circ = 32,739$ Btu per pound mole of dimeric sodium vapor. In their analysis, the thermodynamic function $(F^\circ - H_0^\circ)/T$ for monatomic and diatomic vapor as calculated by Benton and Inatomi (4) was used. The free energy of dimerization is expressed as

$$\Delta F^\circ = \Delta(F^\circ - H_0^\circ) + \Delta H_0^\circ \tag{19}$$

and the equilibrium constant K_p is obtained from

$$K_p = e^{-\Delta F^\circ/RT} \tag{20}$$

and the mole fraction of the species in the equilibrium mixture can be obtained from

$$K_p = \frac{xP}{[(1 - x)P]^2} \tag{21}$$

where x is the fraction dimer and P is the total pressure of the equilibrium mixture. Sodium vapor is assumed to behave ideally. At the normal boiling point (1620° F) the analysis indicates 17 mole

percent dimer, which corresponds to a heat of vaporization to the equilibrium mixture of 1614 Btu per pound. The heat of vaporization to monatomic sodium at 1620° F is 1832 Btu per pound. Hence, errors in the heat of dimerization and therefore in enthalpy of the vapor phase can introduce substantial error in rates of flow calculated by energy balance.

The measured rates of flow were obtained by calculating the volumetric flow from the millivolt output of the magnetic flowmeter by methods described in references 2 and 5 and converting to weight flow using liquid density data. Errors inherent in the calculations and poor control of the liquid level in the accumulator also preclude definite conclusions concerning the critical rates of flow. Entrainment calculations using the method of Langmuir and Blodgett (6) indicate no liquid carryover from the separator; however, due to the lack of a reliable calorimeter and confirmed vapor properties, this cannot be substantiated.

It is apparent that proper investigation of the expansion process of alkali-metal vapors, during restricted as well as critical flow conditions, must be made by directly obtaining reliable and accurate pressure measurements in a convergent-divergent nozzle and accurate measurements of mass flow. Such data with proper analysis will give valuable insight to the effect of the dimerization reaction, supersaturation, and unusual general properties of the metallic vapors in an expansion process.

CONCLUDING REMARKS

The initial operation of the system as discussed here is indicative of the capabilities of the process. Stable system performance was attainable throughout the range of design parameters.

The vapor mass rates of flow through the convergent nozzle as determined by heat balances differ greatly from direct measurements of the condensate. The errors inherent in both methods of determing critical flow rates preclude definite conclusions; however, the critical flow rate is best approximated by a supersaturation expansion assuming ideal gas behavior.

Errors in research data and process control difficulties have been defined and serve as a basis for a separate program to develop instrumentation components for high-temperature two-phase alkali metal systems.

Additional process information and further description of the mechanical and instrumentation aspects of the system are given in reference 7.

NOTATIONS

A	flow area, sq ft
a	flow area, sq in.
C_p	molal specific heat at constant pressure, Btu/(lb-mole)(^oR)
C_v	molal specific heat at constant volume, Btu/(lb-mole)(^oR)
ΔF^σ	change in standard free energy, Btu/(lb-mole)
g_c	conversion constant, 4.17×10^8 (lb_m-ft)/(lb_f-hr^2)
ΔH_0^σ	hypothetical heat of dimerization at absolute zero temperature, Btu/(lb-mole)
h	specific enthalpy, Btu/lb
J	mechanical equivalent of heat, 778 ft-lb/Btu
K_p	equilibrium constant
k	isentropic process constant for a perfect gas, C_p/C_v
M	molecular weight
n	polytropic process constant
P	total absolute pressure, atm
p	total absolute pressure, psia
R	gas constant, Btu/(lb-mole)(^oR)
s	specific entropy, Btu/(lb)(^oR)
T	temperature, ^oR
V	velocity, ft/hr
v	specific volume, cu ft/lb
w	weight flow, lb/hr
x	mole fraction diatomic sodium
y	quality, lb vapor/lb mixture

Subscripts:

c	critical value
f	saturated liquid
g	saturated vapor
m	mixture
p	primary system
s	secondary system
v	vapor
x	variable state point in vapor nozzle
1 to 9	station locations as noted in figure 2

REFERENCES

1. Lyon, R. N., ed., "Liquid-Metals Handbook," Second ed., AEC, 1952.

2. Jackson, C. B., ed., "Liquid-Metals Handbook - Sodium NaK Supplement," Third ed., AEC, 1955.

3. Thomson, G. W., and Garelis, E., "Physical and Thermodynamic Properties of Sodium," Res. Lab. Rep., Ethyl Corp., second ed., Nov. 29, 1955.

4. Benton, A., and Inatomi, T. H., Jour. Chem. Phys., 20, 1946-1948 (1952).

5. Affel, R. G., Burger, G. H., and Pearce, C. L., "Calibration and Testing of 2- and $3\frac{1}{2}$-Inch Magnetic Flowmeters for High-Temperature NaK Service," Rep. 2793, Oak Ridge National Lab., 1960.

6. Langmuir, I., and Blodgett, K., "A Mathematical Investigation of Water Droplet Trajectories," Tech. Rep. 5418, U.S.A.F., 1946.

7. Nichols, L. R., Winzig, C. H., Nosek, S. M., and Goldman, L. J., "Design and Operational Performance of a 150-Kilowatt Sodium Flash-Vaporization Facility." NASA TN D-1661, 1963.

TABLE I. - STEADY STATE DATA

Run number	State point							Measured rates of flow, lb/hr		Electrical power data		
	1	3 or 3'	5	5	6	6'	9					
	Temperature, °F							Primary system, w_p	Secondary system, w_s	kw	amp	volts
	Heater outlet	Separator and nozzle inlet	Vapor chamber	Condenser inlet	Condenser outlet	Accumulator	Heater inlet					
1	1354	1321	1200	1200	1196	1109	1314	12,810	60	57	6,800	10.9
2	1403	1365	1208	1203	1199	1112	1356	12,770	60	67	7,400	11.9
3	1403	1374	1260	1256	1251	1215	1367	18,110	68	67	7,400	11.8
4	1503	1455	1353	1352	1354	1325	1449	18,280	115	93	8,400	13.7
5	1503	1443	1351	1357	1353	1267	1427	12,410	108	94	8,450	13.7
6	1552	1493	1349	1352	1350	1322	1485	16,470	151	108	8,950	14.7
7	1553	1484	1349	1353	1350	1292	1472	12,900	139	107	8,900	14.8
8	1554	1495	1349	1354	1351	1332	1489	16,090	164	108	8,950	14.8
9	1552	1498	1395	1400	1398	1367	1495	18,790	164	107	8,900	14.7
10	1552	1494	1428	1435	1433	1410	1485	15,690	138	105	8,780	14.5
11	1601	1532	1490	1495	1495	1450	1520	14,270	155	114	9,000	15.1
12	1602	1538	1395	1400	1396	1374	1531	18,800	243	127	9,550	15.8
13	1626	1547	1351	1355	1352	1323	1537	15,590	253	137	9,840	16.3
14	1652	1561	1347	1347	1345	1321	1549	15,070	289	148	10,120	16.9
15	1653	1564	1479	1484	1483	1448	1554	14,210	212	143	9,850	16.6
16	1650	1568	1395	1398	1396	1375	1560	16,050	298	145	10,050	16.8
17	1650	1565	1350	1350	1348	1322	1552	15,870	288	150	10,180	17.0
18	1650	1576	1352	1350	1349	1325	1567	18,680	337	149	10,200	17.0
19	1700	1601	1395	1400	1396	1377	1585	16,080	341	167	10,600	18.2

TABLE II. - VAPOR GENERATION RATES

Run	Vapor rate, (lb)/(hr/sq in.)		Nozzle inlet pressure, p_3, psia	Pressure ratio, p_6/p_3
	Calculated from enthalpy balance	Measured		
1	162	129	2.49	0.40
2	184	129	3.36	.30
3	212	145	3.57	.42
4	338	244	5.95	.52
5	287	229	5.51	.56
6	389	318	7.39	.41
7	343	296	7.02	.43
8	370	351	7.48	.41
9	402	350	7.61	.55
10	368	293	7.44	.70
11	390	331	9.51	.79
12	478	516	10.61	.39
13	493	537	9.99	.31
14	544	618	10.78	.27
15	504	452	10.95	.64
16	522	635	11.19	.37
17	539	611	11.01	.27
18	566	720	11.67	.26
19	644	730	13.29	.31

E-1835

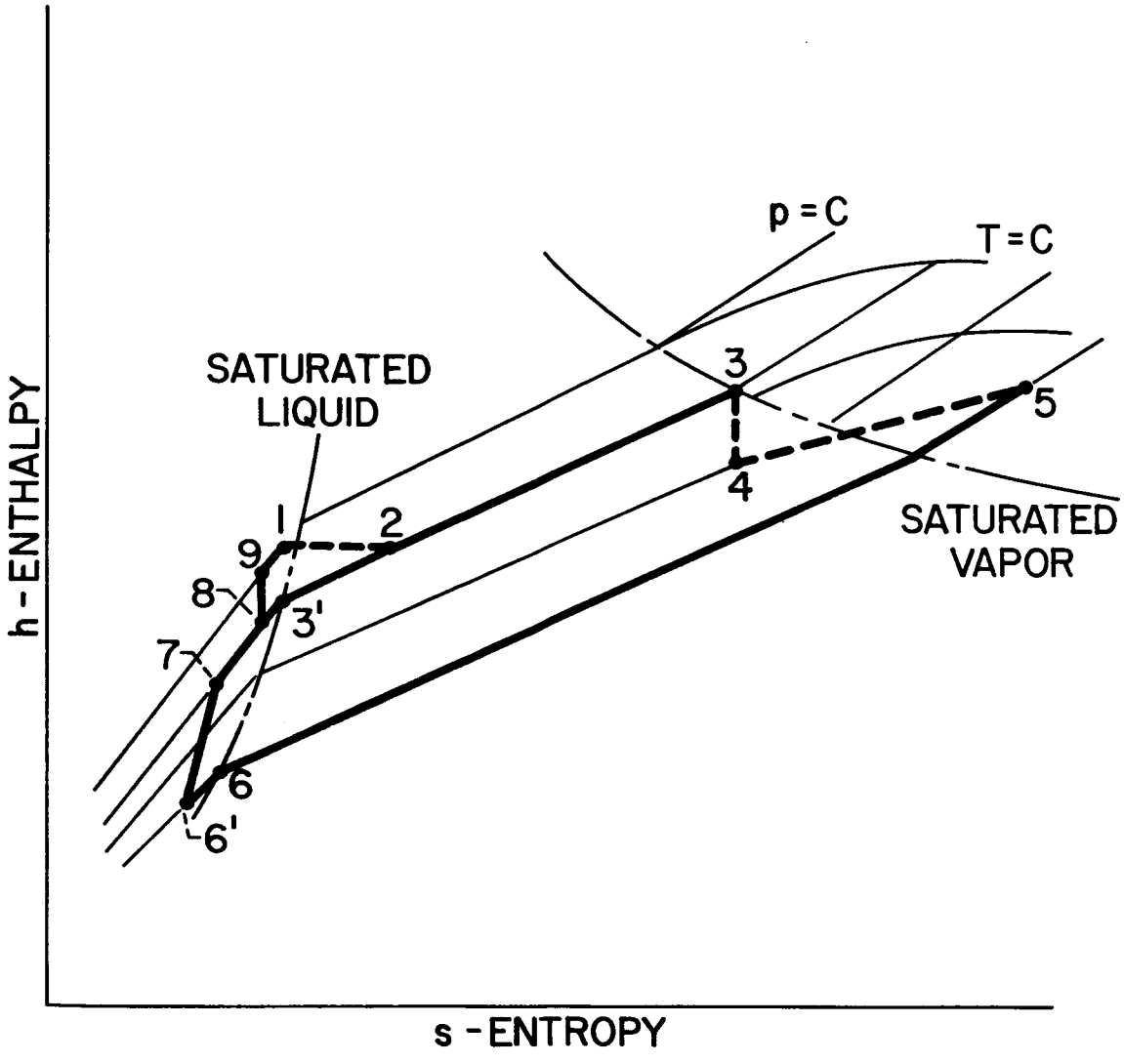

Figure 1. - Thermodynamic cycle of sodium flash vaporization system.

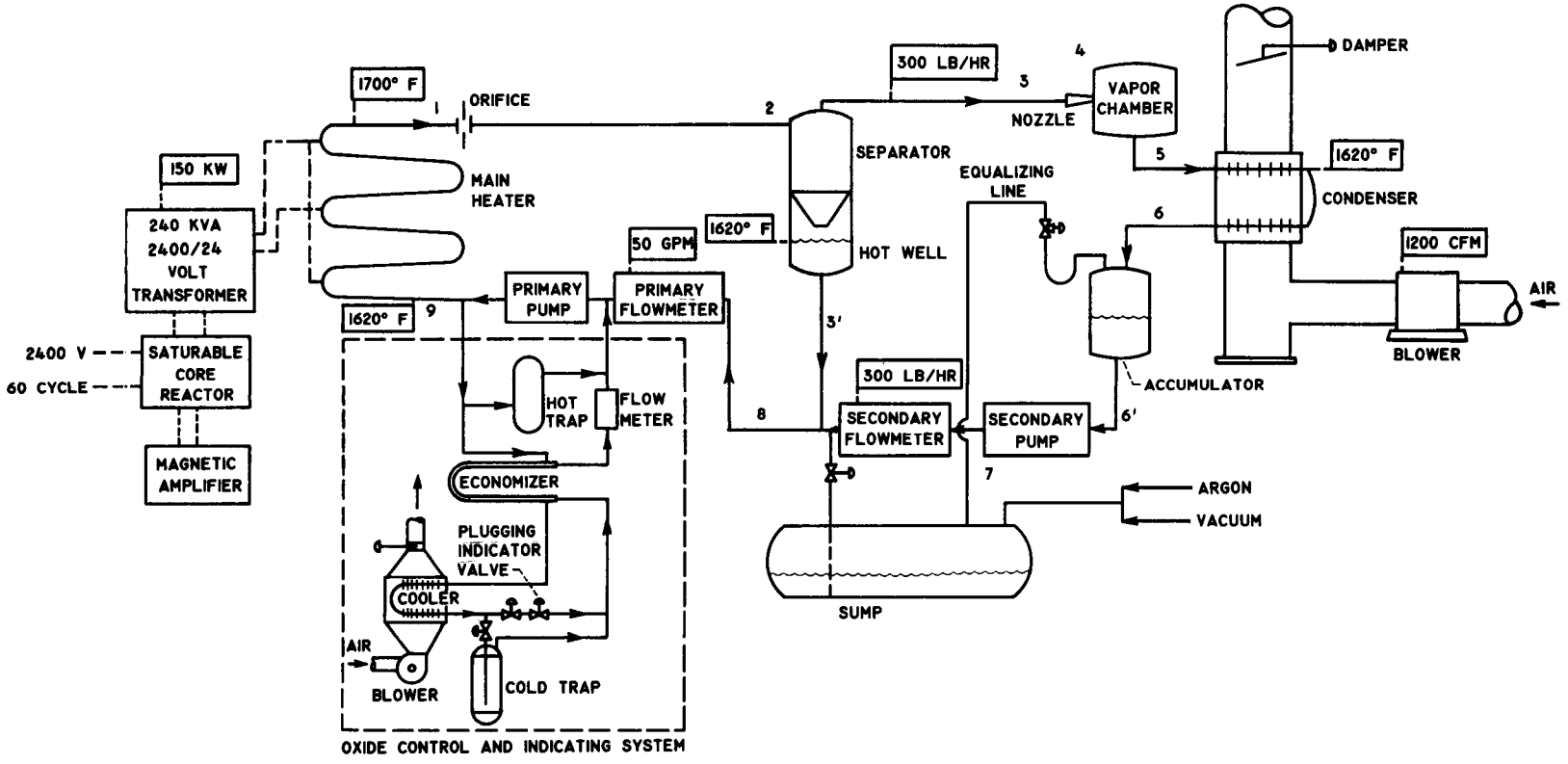

Figure 2. - Schematic of sodium flash vaporization facility.

E-1835

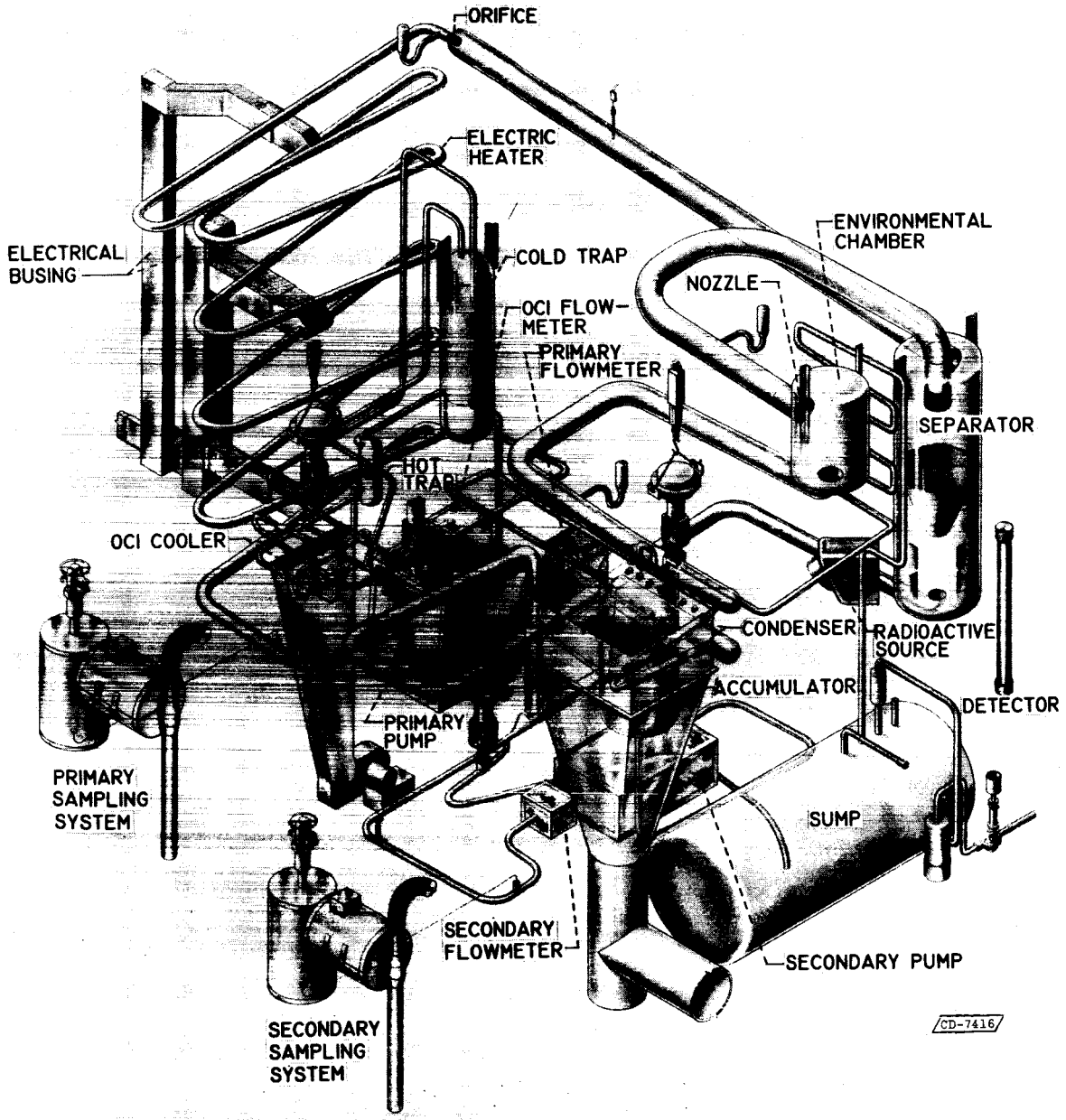

Figure 3. - Isometric of sodium flash vaporization facility.

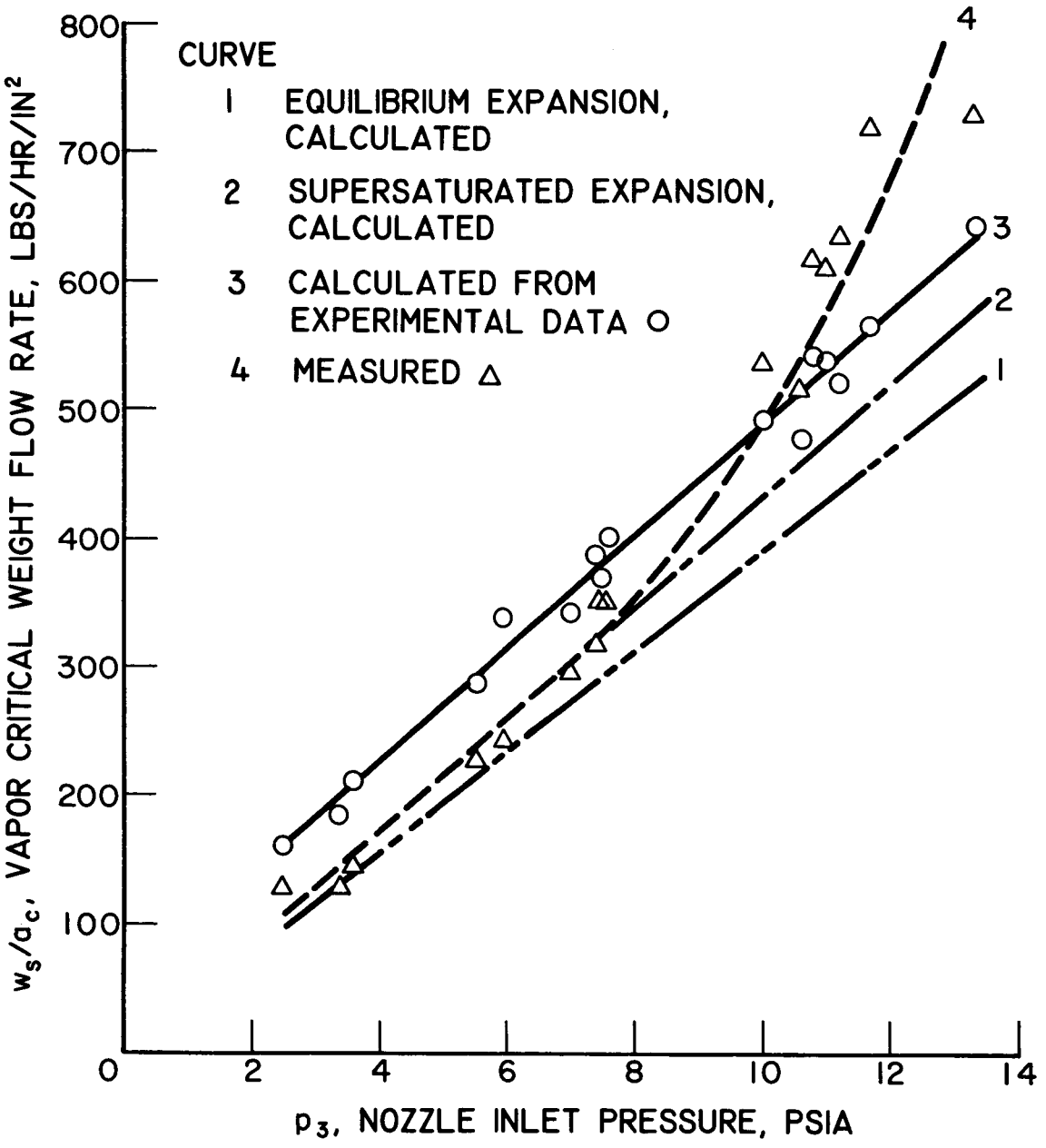

Figure 4. - Variation of vapor critical flow rate with nozzle inlet pressure.